

# Kinetic Monte Carlo Simulation of Underpotential Deposition of Cu on Au(111)

Ryan Stephens

Di Yun

Zhenhua Yu

December 17, 2004

## Under-potential Deposition

The electrochemical deposition of metals on foreign substrates is a complex process which includes a number of phase formation phenomena. The first step of the electrodeposition of a metal(Me) on a foreign substrate(S) is the formation of single Me-adatoms. The adatom-substrate(Me-S) binding energy and the misfit between the crystal lattices of the foreign substrate and the deposit are the most important factors determining the mechanism of the subsequent 2-D and 3-D phase formation processes.

In experiments there are electrodes attached to the substrate, providing electrical potential to assist the deposition. A simple physical consideration tells that if the binding energy of Me-adatoms on the foreign substrate( $\Psi_{Me-S}$ ) is much lower than the adatom binding energy on the own substrate( $\Psi_{Me-Me}$ ), the formation of the 3-D Me-bulk phase in over-potential deposition(OPD) range(the electrode potential  $E$  is negative to the value  $E_{Me/Me^{z+}}$  which characterizes the equilibrium between the 3-D Me-bulk phase and the electrolyte) takes place at relatively low adatom concentrations according to the well known "island growth" mechanism independent of the deposit-substrate crystallographic misfit. However, if  $\Psi_{Me-S} \gg \Psi_{Me-Me}$ , one or several Me-monolayers can be adsorbed in the so-called under-potential deposition(UPD) range( $E > E_{Me/Me^{z+}}$ ).

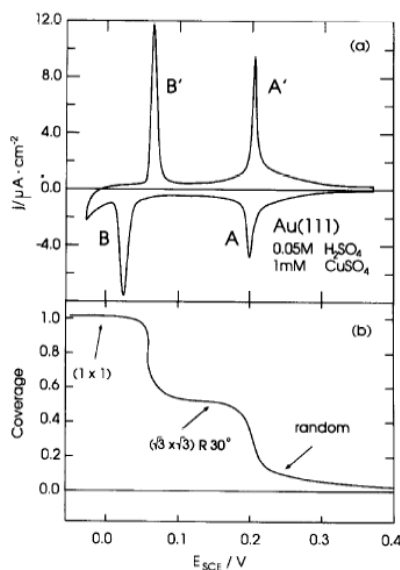


Figure 1: (a) Cyclic current-potential curve for Au(111) in 0.05M  $\text{H}_2\text{SO}_4$  + 1mM  $\text{CuSO}_4$  showing the UPD of Cu (scan rate,  $1\text{mV s}^{-1}$ ). (b) Electrochemically derived Cu coverage (normalized charge due to Cu UPD) as a function of potential, determined by potential steps in the positive direction.

There are already some experiments done to investigate this UPD range. Reference[4] employed the potential-step procedure to study the kinetics of structural changes in the adlayer formed during under-potential deposition of copper on Au(111) in sulphuric acid solution. Basically what they did is to scan the potential of the electrode attached to the Au substrate from high value through the UPD range and measure the current transient (each copper ion deposited to the substrate acquires two electrons and each copper atom desorbed leaves two electrons to the substrate, these processes form the current transient). In Fig.1. the platform in the bottom graph indicates the saturation of the UPD of a monolayer superlattice. Its right edge corresponds to fast UPD process to form the superlattice.

The goal of this present paper is to use kinetic Monte Carlo method to simulate the under-potential deposition of Cu on Au(111).

## Model

The theoretical foundation of dynamical Monte Carlo simulations were laid out long time ago[2]. It turns out a kind of efficient method to simulate the physical phenomena which can be considered as Poisson processes. We employ this method here to study the under-potential deposition.

It is argued that at low coverages the UPD adsorbates usually order in various superlattice structures determined by the substrate matrix, the Me-S misfit and the adatom-adatom interaction. Due to the strong adatom-substrate attraction the formation of these superlattice structures can be considered as localized adsorption which theoretical description corresponds to 2-D lattice gas models equivalent to the Ising model. Therefore the 2-D model proposed by Staikov[1] is believed to capture the physics of the UPD. The following statement of the model is quoted from that paper.

In this model, the elementary rates of single atom adsorption( $k^+$ ) and desorption( $k_i^-$ ) are defined by the expression:

$$k^+ = \begin{cases} k_o e^\beta, & \text{if the site is free} \\ 0, & \text{if the site is occupied} \end{cases} \quad (1)$$

$$k_j^- = k_0 e^{-(j-c/2)\omega} \quad (2)$$

with

$$\beta = -ze(\Delta E - \Delta E^*)/kT \quad (3)$$

$$\omega = \psi/kT \quad (4)$$

$$k_0 = i_{o,ad}(\Delta E^*)\Omega/ze \quad (5)$$

where  $j$  is the actual number of the nearest neighbors of the adatom,  $c$  is the number of the nearest neighbors of an adatom in the compact adlayer,  $\psi$  is the adatom-adatom interaction energy between nearest neighbors,  $\Omega$  is the area corresponding to an adsorption site and  $i_{o,ad}$  is the exchange current density at the reference under-potential  $\Delta E^*$  corresponding to a degree of monolayer coverage  $\theta = 0.5$ . The degree of monolayer coverage  $\theta$  is defined as a relation between the actual and the maximal number of adatoms in the monolayer. It is assumed that the atomic frequency of vibration in the adlayer is the same as in the 3-D bulk crystal, the reference underpotential  $\Delta E^*$  can be defined by the equation

$$ze\Delta E^* = -\Delta\psi_a - \frac{1}{2}c\psi + L_s \quad (6)$$

where  $\Delta\psi_a$  is the energy difference between an occupied and an unoccupied adsorption site, and  $L_s$  is the sublimation energy of the bulk metal. The values we take for these parameters will be given below.

## Algorithm

Our under-potential deposition process can be simulated by kinetic Monte Carlo method. A simple, straightforward way to implement the idea is the following. Select the largest rate  $R_{max}$  of all possible events in our model, deposition or desorption at any site, calculate the relative probabilities  $P_a = R_a/R_{max}$  ( $a$  denotes event  $a$ ) and create the list of possible events in the starting configuration. Then the inner loop of the algorithm in the  $k$ th time step is as follows.

### Algorithm 1

- (i) Randomly select a possible event  $e$  which can be realized in the configuration  $C_k$ .
- (ii) Generate a random number within a uniform distribution of random numbers,  $r \in [0, 1)$ .
- (iii) Compare  $r$  with the probability of the selected event  $P_e$ : if  $r \leq P_e$ , proceed with this event leading to a new state  $C_{k+1} = C'$  and update the list of possible events; if not, stay in the same state.
- (iv) If event  $e$  accepted, advance the real time with  $\Delta t = 1/\sum_a R_a$  ( $R_a$  calculated in the configuration  $C_k$ ); otherwise, the real time doesn't change.

However, this simple algorithm has some shortcomings. If there is a large difference in rates for different events. The low-probability events, once selected, are often rejected. This procedure may lead to many unsuccessful attempts.

The algorithm we use is a modified version of the  $N$ -fold method. Let us group events into  $n$  groups, labelled by  $\alpha = 1, \dots, n$ . This can be done either formally by forming groups with the same number of events, which allows maximal effectiveness of the algorithm, or in a way which keeps the

physics clear: forming groups of the same kinds of events, corresponding to a certain kind of process. We take the latter. Let us have each group represent a certain kind of process, and all events in a group have the same rate  $\rho_\alpha$ .

In a given configuration  $C$ , there are some possible processes, and each kind of possible process can be realized in one or more ways. Assume that a process  $\alpha$  can be realized in  $n_\alpha(C)$  ways, in the configuration  $C$ . We call the quantities  $n_\alpha(C)$  multiplicities. Note conceptually here *process* is different from *event*. To each kind of process we assign a partial rate,  $q_\alpha(C) = n_\alpha(C)\rho_\alpha$ , and a relative probability,  $p_\alpha(C) = q_\alpha(C)/Q(C)$ , which are conditional to the given configuration. The total transition rate in a configuration  $C$  is now  $Q(C) = \sum_{\alpha=1}^n n_\alpha(C)\rho_\alpha$ . In each step of the simulation(in the given configuration) the multiplicities of processes are known. The algorithm in the  $k$ th step of the simulation proceeds as follows.

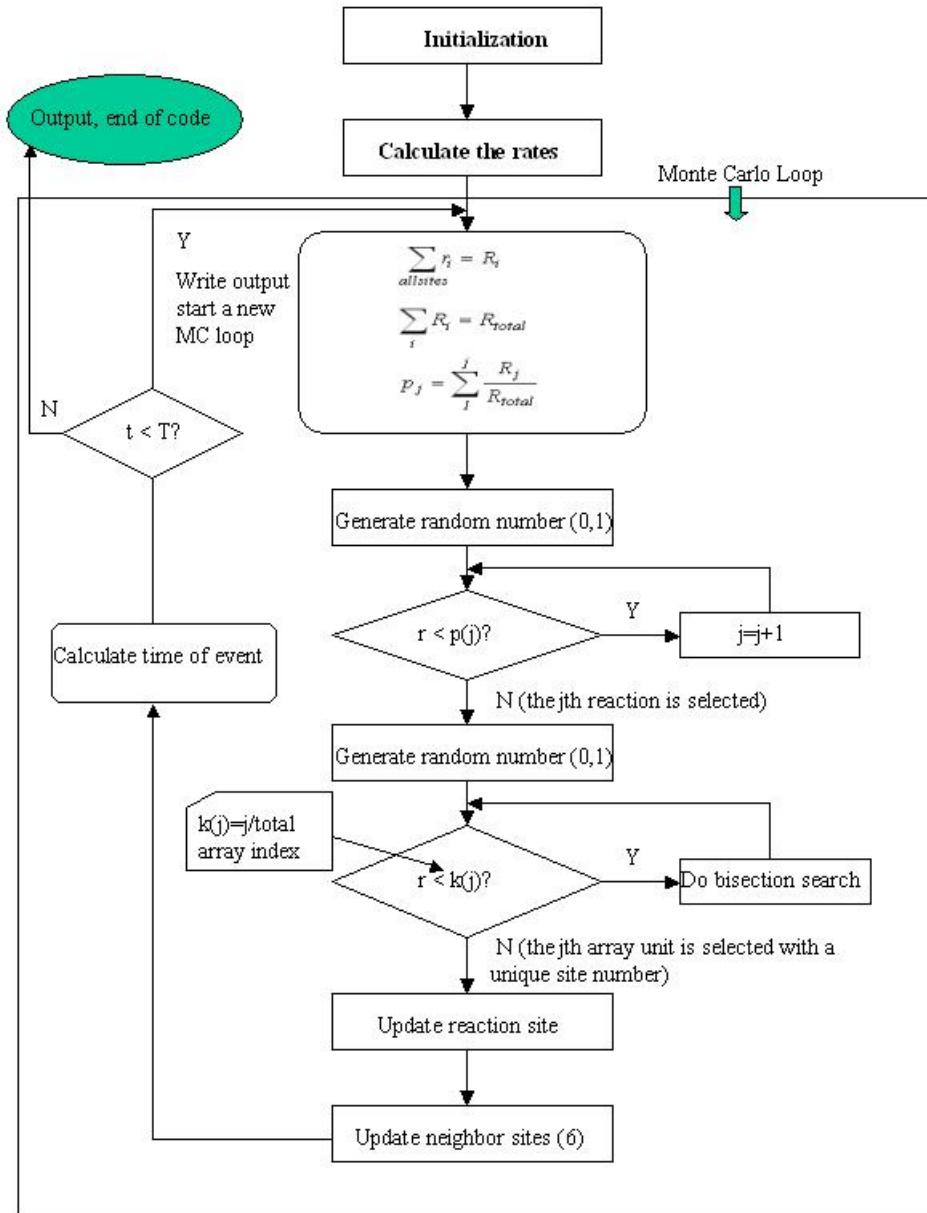
## Algorithm 2

- (i) Choose a random number  $r_1$  in the range  $[0, Q(C_k))$ .
- (ii) Decide which kind of process will take place, choosing the first index  $\sigma$  for which  $\sum_{\alpha=1}^{\sigma} q_\alpha(C_k) \geq r_1$ .
- (iii) Select a realization of the process  $\sigma$ . The  $r_1 \times n_\sigma(C_k)/Q(C_k)$ th event of group  $\sigma$  is selected.
- (iv) Perform the selected event.
- (v) Advance the time with  $\Delta t = 1/Q(C_k)$ .
- (vi) Update the multiplicities  $n_\alpha$ , relative rates  $q_\alpha$ , total rate  $Q$ .

This algorithm does not have the problem that trial movements be rejected. To estimate computer time demands, let us suppose that the multiplicities are approximately the same,  $n_\alpha \approx N/n$  ( $N$  is the number of the sites). The search has two parts: searching for a group, which takes time  $O(N/n)$ , and searching within the group, which takes time  $O(n)$ . Minimizing the total time leads to an optimal number of groups  $n \propto N^{1/2}$ , and the corresponding computer time scales as  $O(N^{1/2})$ . The updating part (vi) may still be  $O(N)$ . Then over all, it scales at most as  $O(N)$ . It turns out to be a very efficient algorithm. The above algorithm discussion is quoted from reference [5].

Following is the detailed description of our code:

## Description of Simulation Code



### 1. Initialization.

Important parameters, arrays and structures:

Interaction Energy:  $\Psi$  we will do a perturbation study of this parameter to see the effect of the potential on the coverage of deposition layer. The results of this study will be presented in the part of simulation result.

Sites structure: generally, it restores the information for each kind of reaction as a separate array of sites.

sites(reaction, index, 1) restores the index of the array unit;  
 sites(reaction, index, 2) restores the site number which uniquely  
 correspond to a site.

Below is a graph shows what's restored in the deposition sites array:

sites array for reaction type 1

site number	index
3764	65
5715	66
496	67
1573	68
3881	69
9290	70
7460	71
6823	72

Rates array: restores 8 basic rates, i.e. adsorption, desorption with no nearest neighbor atoms, desorption with 1 nearest neighbor atom ...

- The calculations of the rates follow the model described by the above sections

$$\sum_{all\ sites} r_i = R_i$$

$$\sum_i R_i = R_{total}$$

$$P_j = \sum_j \frac{R_j}{R_{total}}$$

The probability bin  $p(j)$  will be used to determine which reaction will happen when compared with the random number .

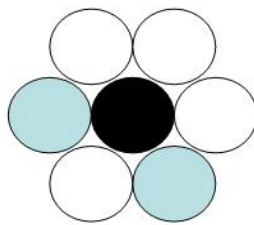
- After the reaction type is decided, we need to decide on which site the reaction happens. To do this, we do a bisection search in the specific reaction sites array mentioned earlier, for instance, if deposition happens, we do a bisection search inside the array of reaction type 1. The bisection search will be considerably faster than the normal search especially when the number of sites is very big.
- Updating the reaction sites is needed since you will need to know the number of neighbor atoms, if the reaction is deposition, to decide which reaction is possible for the reaction atom next time. You will need to eliminate this atom from the

former array and shift the following array units up one unit and clear the last unit of that array and you also need to add this atom into the array which the atom is now belong to. The same thing here for the desorption reaction except it is easier, you don't need to calculate the nearest neighbor atoms. Another thing need to mention is that we apply Periodic Boundary Conditions both for updating the reaction sites and the neighbor sites of reaction sites. The function we use to apply this PBC is the function  $F_x()$  &  $F_y()$  in the code.

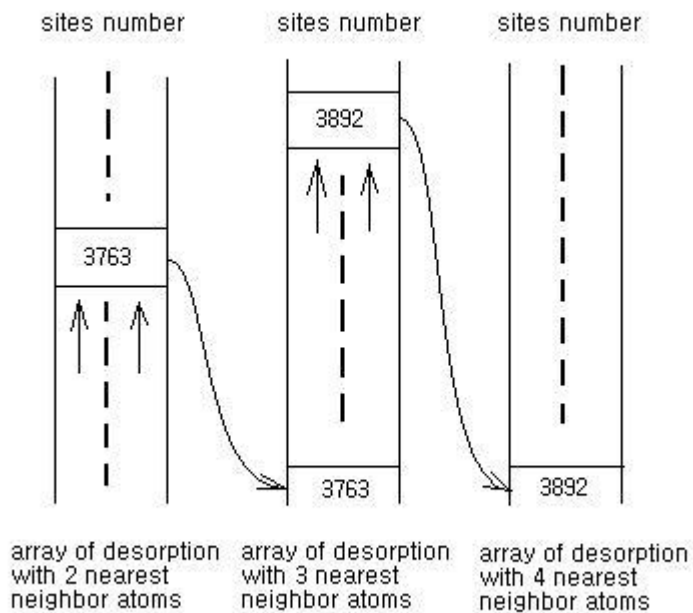
5. The neighbor sites are of our interests when we come to update after the reaction happens. We update these sites using the procedure that follows.

First, do a scan of all the six neighbor sites and find out the array in which these sites are in, or say, what the possible reaction was for these sites before the reaction atom is either deposited or removed nearby.

Then, we need to shift these sites to the neighbor array of reaction according to the reaction type of the reaction atom. For example, if the reaction atom is deposited onto the surface, we will need to shift the sites where there is a copper atom on the surface to an upper reaction type array. The following graphs explain the details of this example.



The black atom is the deposited copper atom, the 2 blue atoms are copper atoms already exist on the surface. Then, after the deposition, these two sites are shifted to the upper 1 reaction type(index) array as shown in the graph below.





The arrows in the graph show the direction of shifting the array units.

6. After finish updating all the sites including the reaction site and the nearest neighbor sites, one Monte Carlo loop is finished, we need to calculate the time incremental according to the formula given by the theoretical model of Kinetic Monte Carlo algorithm  $\Delta t_k = 1/Q(C_k)$ . Then, after the total time  $t_{total} = \sum_k \Delta t_k$  reaches the time line  $T$  set up by the user, the KMC code will end and write the output into output files.

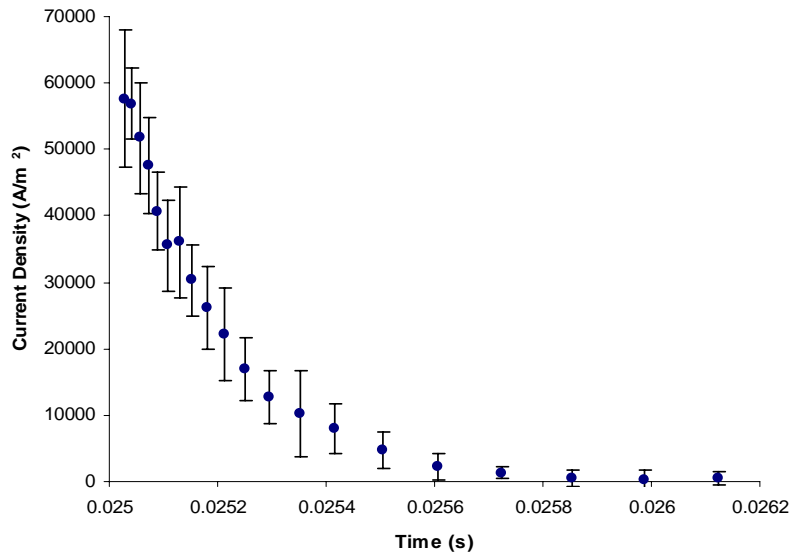
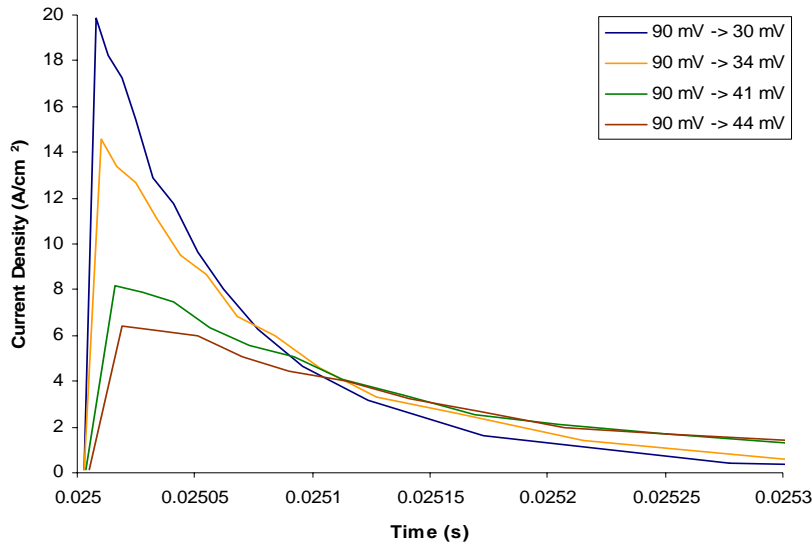
## Results

The code was run to simulate experimental results for two different physical situations: potential steps and potential scans. The computational runs were designed to be compared with experimental results obtained by Holzle et al. The total computational time was estimated to scale as  $O(N^2)$ . Realizing that there are several  $O(N)$  searches in the code, we implemented a bisectional searching method in the part where we use the random number to select the site. This yielded only slight improvement.

The parameters were all obtained from an experimental paper (Holzle et al.) with the exception of the adatom-adatom interaction energy, which was obtained from the theoretical study by Zhang et al. We performed some perturbation studies on this parameter, but saw little difference in the observed trends in the potential step and potential scan calculations. The parameters used are in the following table.

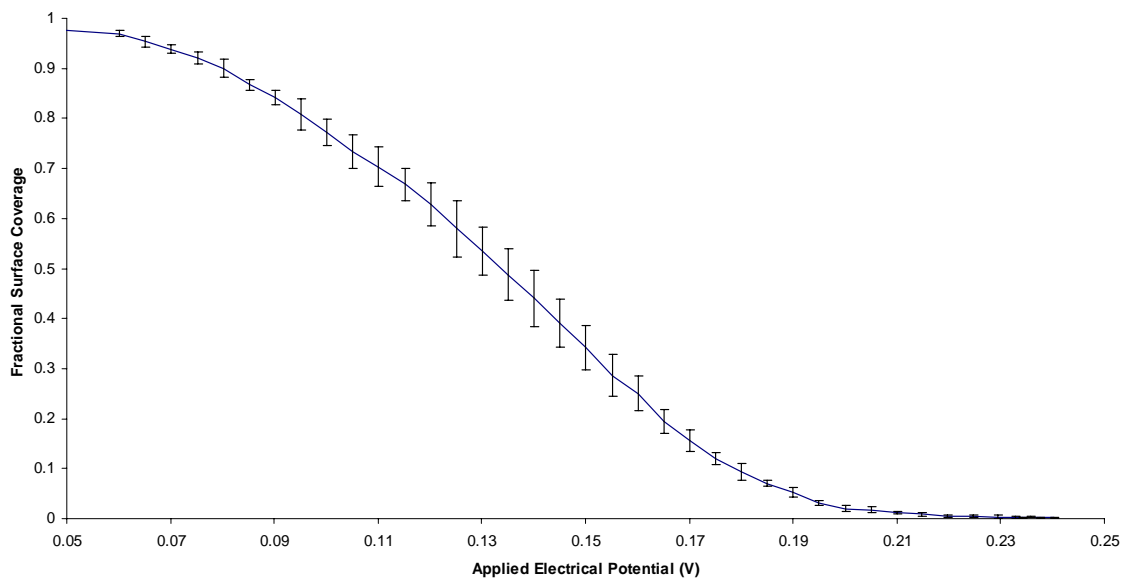
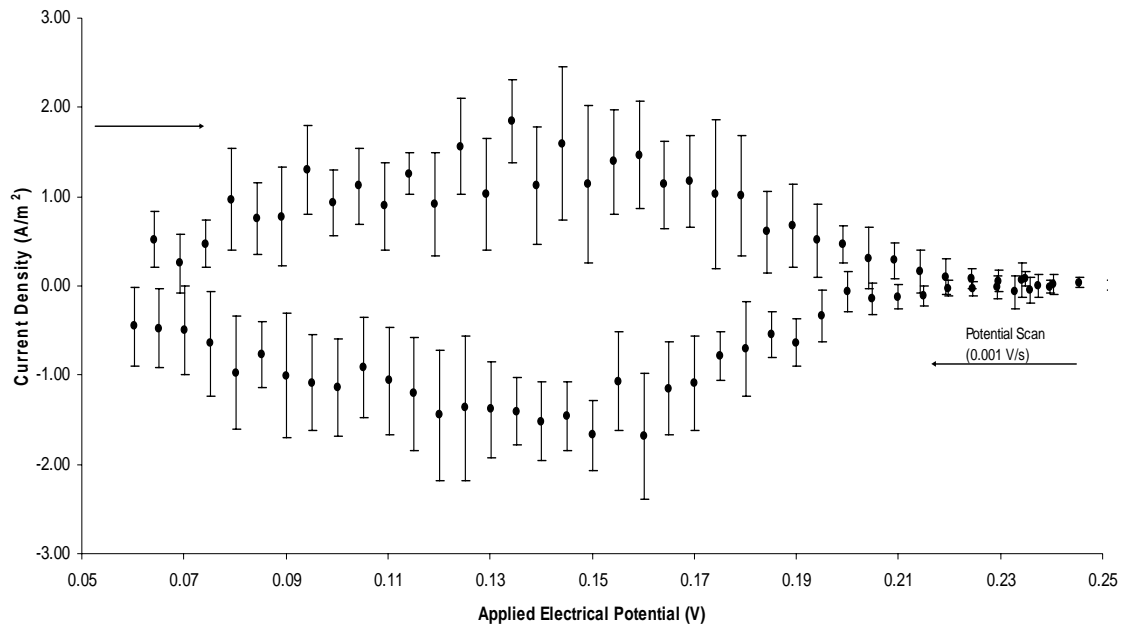
Adatom-adatom interaction energy	$-3 \times 10^{-21}$ J
Exchange current density	11 A/m <sup>2</sup>
Reference underpotential	0.159 V
Area of an adsorption site	$6.5 \times 10^{-20}$ m <sup>2</sup>
Radius of gold atoms	1.442 Angstroms

For potential step experiments, the code was run for until it reached equilibrium at 90 mV (vs. saturate calomel electrode). The potential was then stepped to a lower potential, where the code was run until the system came to equilibrium. The runs were performed for several different step magnitudes. The plots were obtained by averaging the results of ten runs, each using a different seed number for the random number generator. The plot on the bottom shows the step from 90 mV to 44 mV with error bars.

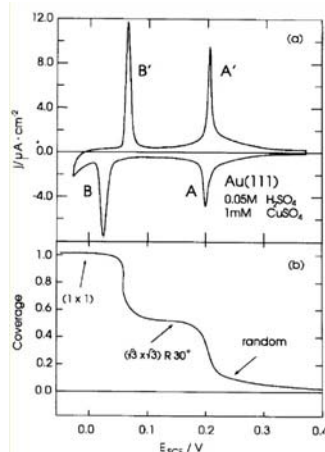


Of specific interest in potential steps in the underpotential region for copper on gold is the appearance of another peak following the initial current peak on the current transient plots. This is noticeably absent in our simulations, and we attribute this to the simplicity of our model. It has been theorized that the experimentally observed peak is due to a nucleation and growth process, which is not accurately represented by our nearest neighbor interaction model, especially without accounting for surface diffusion.

The potential scans were performed by running the code with the potential initially at 25 mV and then reducing the potential until the surface coverage approaches one. At this point, the direction of the potential scan is reversed, and code was run until the surface is clean again. The potential was scanned at a rate of 1 mV per second. The current is plotted over the course of the potential scan. The coverage is also shown as a function of potential.



As with the current transients discussed previously, this cyclic current-potential plot fails to capture all of the behavior observed experimentally. The experimental plots show two distinct current peaks in each direction. The peak which occurs at higher potentials is attributed to formation of a metastable surface ordering, which disappears as the potential decreases. As the potential decreases, remaining unoccupied sites are filled, causing another current peak. A similar pattern is seen when viewing the coverage as a function of potential. Our plots clearly do not show this phase transition.



**Experimental potential scan results (Holzle et al.)**

## Conclusions and Recommendations

After studying the system using this simplified model, we conclude that a more complicated approach must be taken in order to observe these phase transitions. In our model, the interaction energy between atoms was only taken into consideration when calculating the rates of desorption. In order for the surface energetics to play a larger role, the interaction energies must be applied to the rate of movement into a site, not just to the rate for leaving a site. This could be done through making certain sites more favorable for adsorption and/or implementation of surface diffusion. Surface diffusion in particular would allow the surface to reach a state that is more favorable energetically.

Another possibility for improving the accuracy of the calculations would be to implement a more realistic interaction potential, instead of just nearest neighbor repulsions. A better model should also account for coadsorption of anions, which would give a more realistic picture of the surface under these experimental conditions.

There are also possibilities for improving the algorithm. The most computationally expensive step is probably updating the neighbor sites after each reaction. Rather than searching through the list of sites to find out what reactions they are currently configured to undergo, it may be possible to use other arrays to store those sites and eliminating the need for that  $O(N)$  search.

## References:

1. G. Staikov, in *Nanoscale Probes of the Solid/Liquid Interface*, edited by A.A. Gewirth and H. Siegenthaler, Kluwer Academic Publishers, The Netherlands, (1995).
2. K. A. Fichthorn and W. H. Weinberg, *J. Chem. Phys.*, 95, 1090-1096 (1991).
3. J. Zhang, Y. Sung, P. Rikvold, and A. Wieckowski, *J. Chem. Phys.*, 104, 5699-5712 (1996).
4. M. H. Holzle, U. Retter, and D. M. Kolb, *J. Electroanalytical Chem.*, 371, 101-109 (1994).
5. A. C. Levi and M. Kotrla, *J. Phys.: Condens. Matter*, 9, 299-344 (1997).